Experimental Verification of Nondiffracting X Waves

Jian-yu Lu, *Member, IEEE* and James F. Greenleaf, *Fellow, IEEE*

Abstract—**The authors have embedded descriptions for localized nondiffracting waves such as Durnin's wave in a generalized family of exact solutions to the isotropic/homogeneous wave equation. The first experimental production of acoustic forms of a subset of these solutions that the authors term, "X waves" are reported. Our generalized expression includes a term for the frequency response of the system and parameters for varying depth of field versus beam width of the resulting family of beams. Excellent agreement between theoretical predictions and experiment was obtained. An X wave of finite aperture driven with realizable (causal, finite energy) pulses travels with a large depth of field (nondiffracting length).**

I. Introduction

THE PROPAGATION of acoustic waves in isotropic/homogeneous media and electromagnetic waves in free space is governed by the isotropic/homogeneous (or free space) scalar wave equation. The first localized solution of the free-space scalar wave equation was discovered by J. N. Brittingham in 1983 and was called a focus wave mode [1]. In 1985, R. W. Ziolkowski discovered a new localized solution of the free-space scalar wave equation and found a way to construct new solutions from this localized solution by Laplace transform [2]. In 1989, a localized solution using the so-called modified power spectrum was constructed and the predicted localized wave was experimentally realized through acoustical superposition [3]. These localized solutions were further studied by several investigators [4]–[10].

The first nondiffracting beam that was an exact solution of the free-space scalar wave equation was discovered by J. Durnin in 1987 [11]. A finite aperture approximation of this beam was expressed in continuous wave form and was realized by optical experiments (treating the scalar amplitude of one transverse component of either the electrical or magnetic field as the solution of the scalar wave equation) [12]. Durnin's beams were further studied in optics in a number of papers [13]–[19]. Hsu *et al.* [20] realized a J_0 Bessel beam with a narrow-band PZT ceramic ultrasonic transducer of nonuniform poling. We made the first J_0 Bessel annular array transducer [21] using a PZT ceramic/polymer composite and applied it to medical acoustic imaging and tissue characterization [22]–[25]. Campbell *et al.* had a similar idea to use an annular array to realize a J_0 Bessel beam and compared the J_0 Bessel beam to the Axicon [26].

Manuscript received August 21, 1991; revised and accepted January 3, 1992. This work was supported in part by grant CA 43920 from the National Institutes of Health.

The authors are with the Biodynamics Research Unit, Department of Physiology and Biophysics, Mayo Clinic and Foundation, Rochester, MN 55905

IEEE Log Number 9107528.

We have recently discovered families of generalized nondiffracting solutions of the free-space scalar wave equation [27]. One subset of these solutions represents waves that have X-like shapes in a plane along the axis of the waves and we term them "X waves" [27]. The nondiffracting X waves propagate without changing their waveforms in both space and time provided they are produced by an infinite aperture. Even with finite aperture, nearly exact X waves can be realized with either broadband or band-limited radiators over deep depth of field (nondiffracting distance). In comparison with Durnin's beam [11], X waves contain multiple frequencies and are localized in both space and time. X waves are nondiffracting in nature and have a constant peak amplitude as they propagate. This is different from Brittingham's [1] and Ziolkowski's [2], [3] localized waves that recover their amplitude periodically or aperiodically.

In this paper, we report the experimental production of an axially symmetric acoustic X wave and compare it with computer simulations.

II. Theoretical Preliminaries

The isotropic/homogeneous scalar wave equation in cylindrical coordinates is given by

$$\left[\frac{1}{r}\frac{\partial}{\partial r}\left(r\frac{\partial}{\partial r}\right)+\frac{1}{r^2}\frac{\partial^2}{\partial\phi^2}+\frac{\partial^2}{\partial z^2}-\frac{1}{c^2}\frac{\partial^2}{\partial t^2}\right]\Phi=0 \quad (1)$$

where $r=\sqrt{x^2+y^2}$ represents radial coordinate, ϕ is the azimuthal angle, z is the axial axis, which is perpendicular to the plane defined by r and ϕ, t is the time, c is the speed of sound, and Φ represents acoustic pressure that is a function of r, ϕ, z, and t. One of the families of generalized solutions of (1) discovered recently by us [27] is of the form

$$\Phi_\zeta(s)=\int_0^\infty T(k)\left[\frac{1}{2\pi}\int_{-\pi}^{\pi}A(\theta)f(s)d\theta\right]dk \quad (2)$$

where

$$s=\alpha_0(k,\zeta)r\cos(\phi-\theta)+b(k,\zeta)[z\pm c_1(k,\zeta)t] \quad (3)$$

and where

$$c_1(k,\zeta)=c\sqrt{1+[\alpha_0(k,\zeta)/b(k,\zeta)]^2}. \quad (4)$$

where $T(k)$ can be any complex function (well behaved) of k ($k=\omega/c$ is a wave number and ω is angular frequency) and could include the frequency response of an acoustic transducer. $A(\theta)$ is any complex function (well behaved) of θ and represents a weighting function of the integration with respect to θ, which is the angle around the aperture of the

transducer, $f(s)$ is any complex function (well behaved) of s, $\alpha_0(k,\zeta)$ is any complex function of k and ζ, $b(k,\zeta)$ is any complex function of k and ζ, and k and ζ $(0 < \zeta < \pi/2)$ are parameters that are independent of the spatial and time variables (r, ϕ, z, and t) of $\Phi_\zeta(s)$.

If $c_1(k,\zeta)$ in (3) is real and independent of the wave number, k, $\Phi_\zeta(s)$ in (2) represents a family of complex waves that are nondispersive, the peak of which will travel with speed c_1 in isotropic/homogeneous media without changing wave shape in either transverse or axial directions. This means that the waves represented by (2) are nondiffracting, i.e., both the phase and amplitude of the complex wave are kept unchanged in space and time as the wave propagates.

Although the peak of the wave travels with speed c_1, which is greater than the speed of sound c, the individual components do not travel faster than c nor do the wave fronts in the realizable finite aperture case. More detailed discussion of the wave peak speed, c_1, is reported in [27].

If in (2), we let $f(s) = e^s$, $A(\theta) = i^n e^{in\theta}$, $\alpha_0(k,\zeta) = -ik\sin\zeta$, $b(k,\zeta) = ik\cos\zeta$, $T(k) = a_0 e^{-a_0 k}$, and use the "-" term in (3), we obtain the nth order forward going (along positive z direction) broadband nondiffracting X wave [27]:

$$\Phi_{XBB_n} = \frac{a_0(r\sin\zeta)^n e^{in\phi}}{\sqrt{M}\left(\tau+\sqrt{M}\right)^n}, \quad (n = 0, 1, 2, \ldots) \tag{5}$$

where subscript BB means broadband, $M = (r\sin\zeta)^2 + \tau^2$, and where $\tau = [a_0 - i(z\cos\zeta - ct)]$, and $a_0 > 0$ is a constant. Because $T(k)$ is free to choose, it can be used to represent band-limited waves. For instance, if $T(k) = B(k)e^{-a_0 k}$, where $B(k)$ is any band-limited complex function (well-behaved) that represents a system transfer function of a practical transducer, we obtain the nth order band-limited X waves [27]:

$$\Phi_{XBL_n} = \frac{1}{a_0}\mathcal{F}^{-1}\left[B\left(\frac{\omega}{c}\right)\right] * \Phi_{XBB_n}, \ (n = 0, 1, 2, \ldots) \tag{6}$$

where the subscript BL represents "band-limited," the symbol * denotes the time convolution and $\mathcal{F}^{-1}$ represents the inverse Fourier transform.

The X waves ((5) and (6)) travel to infinite distance at speed of $c/\cos\zeta$ in isotropic/homogeneous media (or free space) without changing shape in any direction, provided that they are produced by an infinite aperture. For $n = 0$ (zeroth order), one obtains axially symmetric X waves, Φ_{XBB_0} and Φ_{XBL_0}.

In practical applications, causal, finite bandwidth signals, and finite apertures must be used to approximate the theoretical results of (5) and (6). In this case, the X waves are nondiffracting over a finite distance (−6-dB depth of field) that is given by [27]:

$$Z_{\max} = \frac{D}{2}\cot\zeta \tag{7}$$

where D is the diameter of the aperture. For the zeroth-order broadband X wave, the −6-dB lateral (BW_L) and axial (BW_A) beam widths of $|\Phi_{XBB_0}|$ are; $BW_L = 2\sqrt{3}a_0/|\sin\zeta|$ and $BW_A = 2\sqrt{3}a_0/|\cos\zeta|$, [27]. The subscripts L and A mean "lateral" and "axial," respectively.

III. Simulations and Experiments

We demonstrate the feasibility of producing a zeroth-order (axially symmetric), band-limited X wave with a finite aperture and causal pressure pulses by comparing beam simulations of a physical ultrasonic transducer to measurements of its experimental beam.

A. Simulations

Panels (1) and (2) in Fig. 1 present computer simulations of the zeroth-order, band-limited, and finite-aperture X wave pressure distributions ($n = 0$ in (6)) at distances z =170 mm and 340 mm, respectively, away from the surface of a 50-mm diameter transducer. The simulations were performed using the Rayleigh–Sommerfeld formulation of diffraction [28] and an exact X wave shading. The transmitting transfer function of the transducer $B(k)$ in (6) was approximated with a Blackman widow function [29] peaked at 2.5 MHz with −6-dB bandwidth around 2.1 MHz with the following form:

$$B(k) = \begin{cases} a_0\left[0.42 - 0.5\cos\dfrac{\pi k}{k_0} + 0.08\cos\dfrac{2\pi k}{k_0}\right], & 0 \le k \le 2k_0 \\ 0, & \text{otherwise} \end{cases} \tag{8}$$

where $k_0 = 2\pi f_0/c$ and f_0 =2.5 MHz. For the simulations we used a broadband X wave pressure pulse drive over the 50-mm aperture of the transducer.

B. Experiments

Corresponding to the simulations, Panels (3) and (4) in Fig. 1 show the experimentally measured pressure waves at distances z = 170 mm and 340 mm, respectively. The experimental transducer used to produce the X waves was an annular array transducer made of PZT ceramic/polymer composite and had annular rings cut on the lobes of a J_0 Bessel function [21], [22]. The transducer has 10 elements with a maximum diameter of 50 mm and had a central frequency of 2.5 MHz. Its −6-dB pulse–echo bandwidth is about 50% of the central frequency. The panel size of Fig. 1 is 25 mm × 10 mm, and the parameters a_0 and ζ are 0.05 mm and 4°, respectively. The linear analytic envelope of the real part of the X waves is displayed.

The experiment was done as follows. A block diagram of the experimental system for producing acoustic zeroth order (axially symmetric) X waves is shown in Fig. 2. A polynomial waveform synthesizer (Model 2045) was used to generate 10 broadband X wave drive functions for the 10 transducer elements. The broadband X wave drive functions were calculated from the real part of (5) with both n and z set to zero. The radius r used for the calculation of the pulse for each ring was the average radius of each transducer element [21], and the drive function was truncated at ±5 μs (see Fig. 3). The X wave drive pulses were amplified by an RF power amplifier with its output coupled through a 16:1 impedance reduction transformer to improve the fidelity of

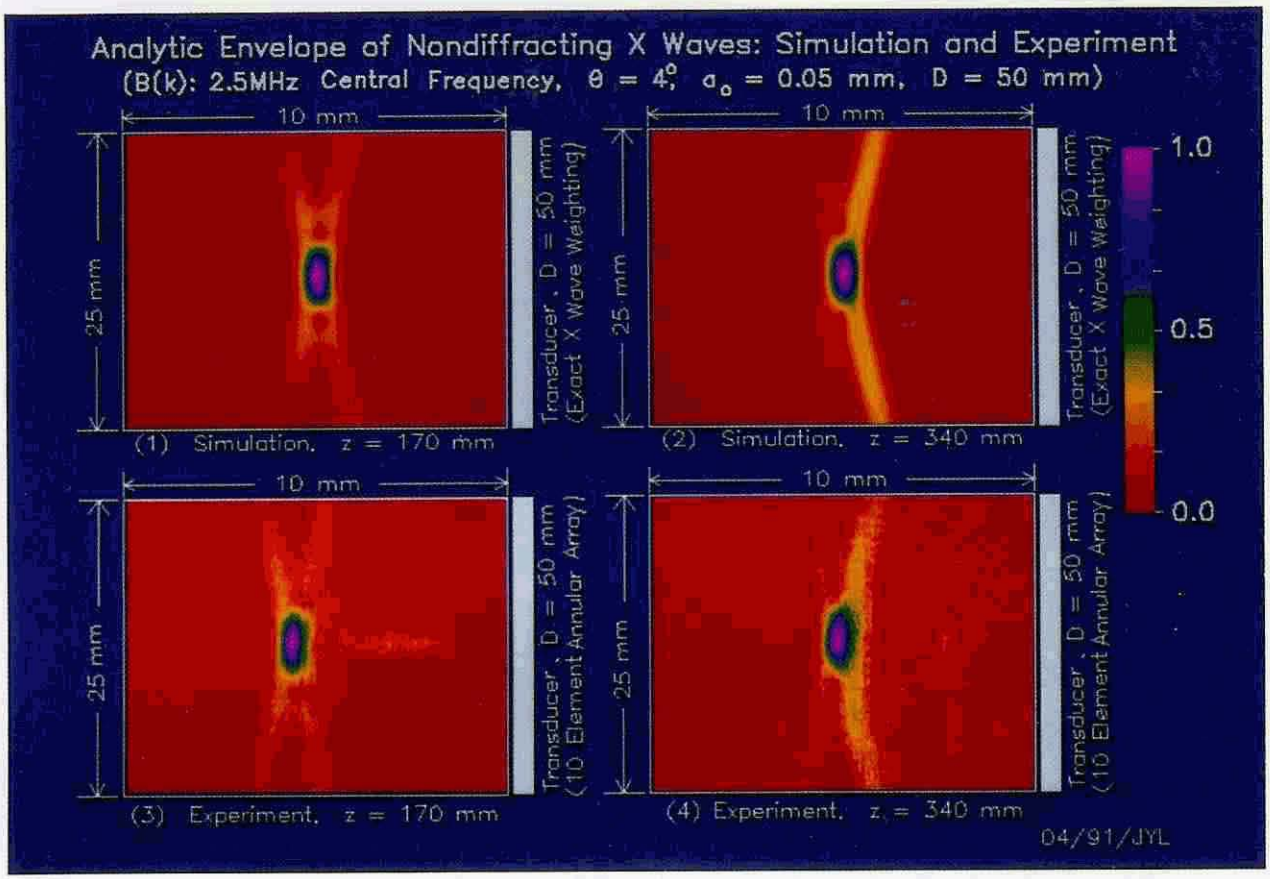

Fig. 1. Panels (1) and (2): Computer simulations of the zeroth-order ($n = 0$) band-limited X wave at distances z =170 mm and 340 mm, respectively, away from the surface of a 50-mm-diameter transducer. An exact X wave aperture shading and a broadband X wave pulse drive of the transducer were assumed. The transmitting transfer function of the transducer was assumed to be the Blackman window function peaked at 2.5 MHz and with −6-dB bandwidth around 2.1 MHz (see (8)). Panels (3) and (4): Experimental results that correspond to the simulations in (1) and (2), respectively. A 10-element, 50-mm-diameter, 2.5-MHz central frequency, PZT ceramic/polymer composite J_0 Bessel transducer [21], [22] with a −6-dB pulse–echo bandwidth about 50% of the central frequency was used. The panel size is 25 mm × 10 mm, and the parameters a_0 and ζ are 0.05 mm and 4°, respectively. Linear analytic envelope of the real part of the X wave is displayed in all panels.

the drive waveforms. The transducer was excited one annulus at a time and the acoustic waves were measured in water in a plane along the axis of the transducer with a 0.5-mm diameter calibrated hydrophone and digitized at 40 megasamples/s. The measured RF signals produced by the 10 transducer elements were summed. Excitation of the transducer and acquisition of data were synchronized to the scan of the hydrophone and were controlled by a minicomputer.

Fig. 4 shows the lateral (Figs. 4(a1) and (a2)) and axial (Figs. 4(a3) and (a4)) beam plots of the X waves in Fig. 1 at distances z = 170 mm (Figs. 4(a1) and (a3)) and 340 mm (Figs. 4(a2) and (a4)). We simulated the experimental piecewise X wave aperture by dividing the transducer into 10 annuli corresponding to the annular cuts of the experimental transducer. The annuli were driven with the same 10 broadband X wave drive functions used for the experiment. Fig. 4(b) shows calculated peak magnitudes of the X wave along the axial axis z of the transducer, from 10 mm to 700 mm. The * symbol represents the points where the X wave profiles were measured experimentally.

Fig. 4 shows that the X wave has a −6-dB depth of field of about 349 mm (dotted line in Fig. 4(b)). The −6-dB depth

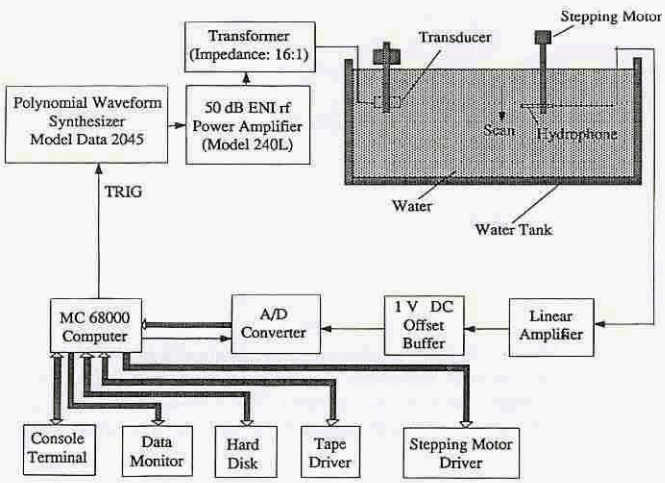

Fig. 2. Block diagram of acoustic production of the zeroth-order (axially symmetric) X wave.

of field calculated from the theoretical predication, $Z_{\max}$ in (7), is about 358 mm, which is very close to what we simulated and measured (see Fig. 4(b)). The −6-dB lateral and axial beam widths of the experimental band-limited X

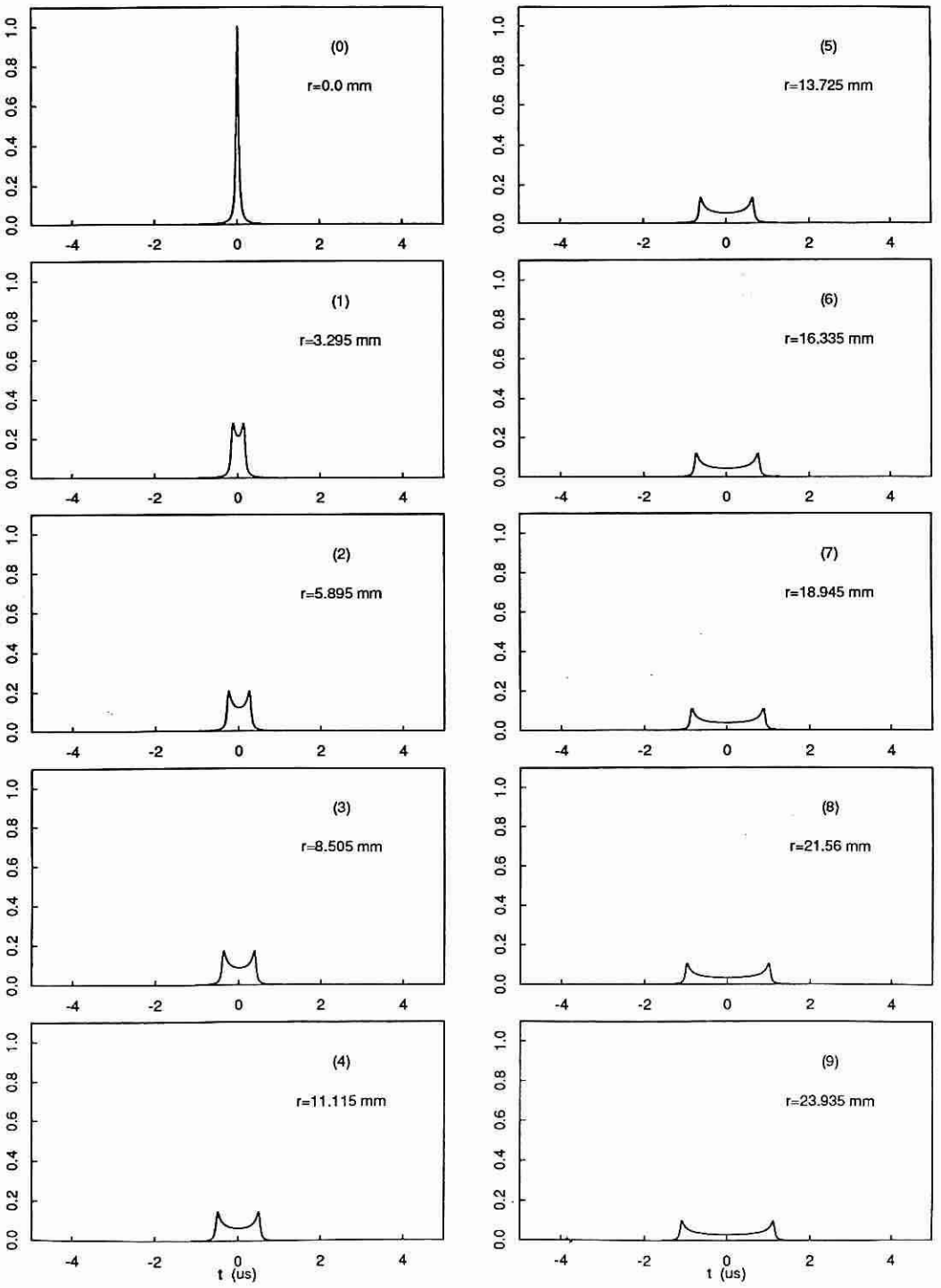

Fig. 3. Ten electrical waveforms (obtained from (5) when both n and z were set to zero) for driving the ten elements of the acoustic annular array transducer to produce the piecewise approximated X wave. The waveforms are calculated with radii r equal to the average radius of each element. The waveforms are truncated at $\pm 5\mu$s. (0)–(9) are drive functions for transducer elements from innermost to outmost, respectively, and are normalized to the amplitude of the drive function in (0).

wave (2.5-MHz central frequency) are about 4.7 mm and 0.65 mm, respectively, throughout the depth of field. The Rayleigh distance of an unfocused Gaussian beam with the same −6-dB lateral beam width is only about 28.9 mm at a frequency of 2.5 MHz in water even if it is produced by an infinite aperture! A general description of nondiffracting and diffracting beams and the relationship among aperture size, lateral beam width and the depth of field of beams is given in [30].

The high peak pressure of the X wave near the surface of the transducer resulted from the piecewise approximation of the transducer aperture (10 annular elements in our experiment) and was predicted by the simulation (see dashed line in Fig. 4(b)). Although the X wave has a narrow lateral beamwidth through its peak (wave center), it has X branches (see Fig. 1)

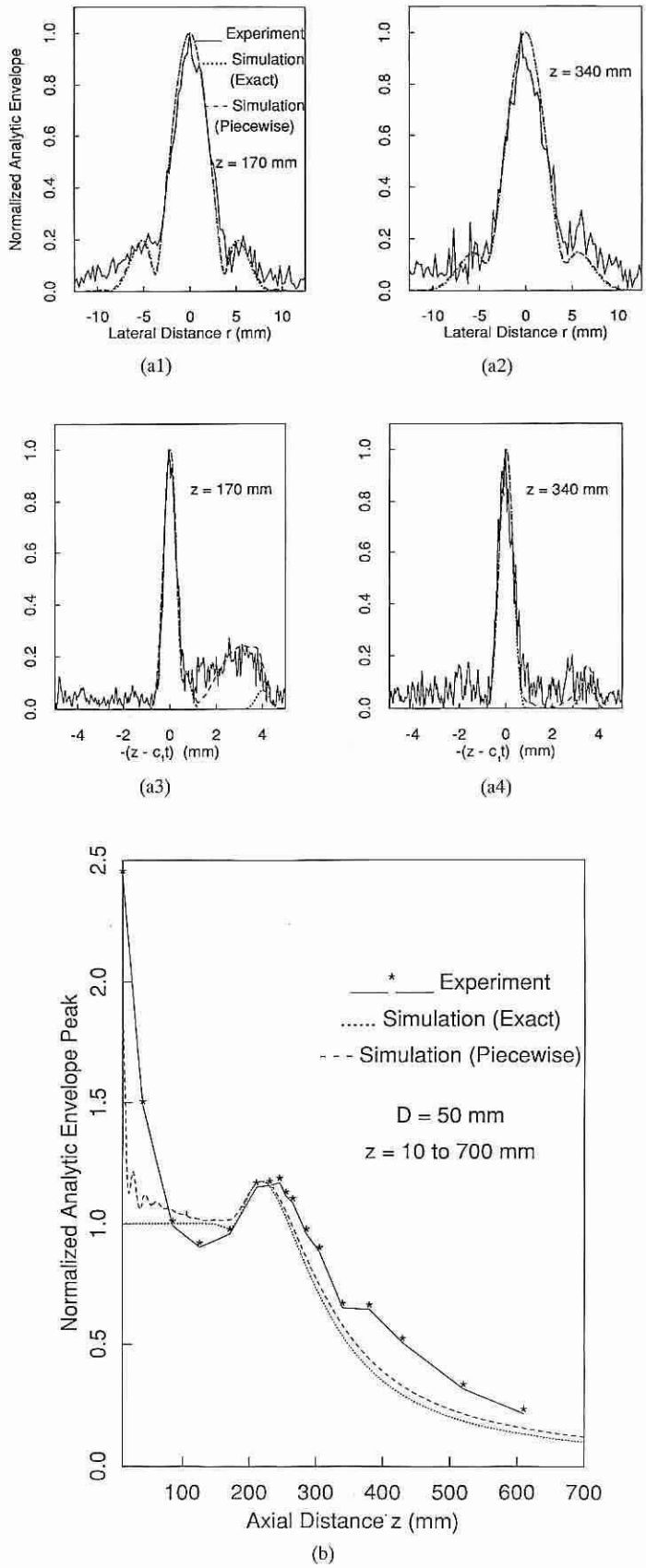

Fig. 4. Lateral ((a1) and (a2)) and axial ((a3) and (a4)) beam plots of the X waves in Fig. 1 at distances $z = 170$ mm ((a1) and (a3)) and 340 mm ((a2) and (a4)). Full lines, dotted lines, and dashed lines correspond to experiment, simulations with an exact X wave aperture shading and simulations with a piecewise X wave aperture shading, respectively. (b) Peak magnitude of the X wave along the axial axis, z, of the transducer, from 10 mm to 700 mm.

that can be treated as sidelobes in imaging. The effects of the X branches in imaging could be reduced by using a combination of X wave transmitting and conventional dynamic spherically focused receiving, which could produce high resolution, high-contrast pulse–echo imaging at high frame rate within the large depth of field of the X wave. More discussion on sidelobes of X waves are found in [27], [30].

The experimentally measured values agree closely with the simulation results (Figs. 1 and 2). The X wave is almost exactly realized over a large depth of field. This demonstrates that although the exact nondiffracting X waves ((5) and (6)) may not be physically realizable (not causal and do not have finite total energy [27]), they can be well approximated with finite aperture physical devices and with causal pressure pulses [27] (truncated at ± 5 μs relative to the peak of the wave in our experiments) over a large distance (of course, the finite aperture device produces a finite depth of nondiffraction). As with the J_0 Bessel beam, X waves could be applied to acoustic imaging and tissue characterization [21]–[25]. As with Ziolkowski's localized waves [7], X waves could be used for electromagnetic energy transmission, private communication and military systems, etc.

IV. Conclusion

We have discovered a novel family of nondiffracting waves. We call one subset of this family "X waves" because they have X-like shapes in a plane along their wave axis. A zeroth order acoustic X wave (axially symmetric) was experimentally produced with an acoustic annular array transducer. The experimental results matched theoretical predictions.

Like Durnin's beams [11], X waves could find applications in acoustic imaging for increasing depth of field [21], [22], [24], [25]. Tissue characterization could be simplified without the need for diffraction compensation due to beam spreading [23]. X waves could also have applications in electromagnetic energy transmission [7].

Acknowledgment

The authors appreciate the help of Thomas M. Kinter in developing software for data acquisitions. The authors also appreciate the help of Randall R. Kinnick in making transformers to drive the transducer. The authors appreciate the secretarial assistance of Elaine C. Quarve and the graphic assistance of Christine A. Welch.

References

[1] J. B. Brittingham, "Focus wave modes in homogeneous Maxwell's equations: transverse electric mode," *J. Appl. Phys.*, vol 54, no. 3, pp. 1179–1189, 1983

[2] R. W. Ziolkowski, "Exact solutions of the wave equation with complex source locations," *J. Math. Phys.*, vol. 26, no. 4, pp. 861–863, Apr. 1985

[3] R. W. Ziolkowski, D. K. Lewis, and B. D. Cook, "Evidence of localized wave transmission," *Phys. Rev. Lett.*, vol. 62, no. 2, pp. 147–150, Jan. 9, 1989

[4] A. M. Shaarawi, I. M. Besieris, and R. W. Ziolkowski, "Localized energy pulse train launched from an open, semi-infinite, circular waveguide," *J. Appl. Phys.*, vol. 65, no. 2, pp. 805–813, 1989

[5] I. M. Besieris, A. M. Shaarawi, and R. W. Ziolkowski, "A bidirectional traveling plane wave representation of exact solutions of the scalar wave equation," *J. Math. Phys.*, vol. 30, no. 6, pp. 1254–1269, 1989

[6] E. Heyman, B. Z. Steinberg, and L. B. Felsen, "Spectral analysis of focus wave modes," *J. Opt. Soc. Amer. A*, vol. 4, no. 11, pp. 2081–2091, Nov., 1987
[7] R. W. Ziolkowski, "Localized transmission of electromagnetic energy," *Phys. Rev. A.*, vol. 39, no. 4, pp. 2005–2033, Feb. 15, 1989
[8] J. V. Candy, R. W. Ziolkowski, and D. K. Lewis, "Transient waves: reconstruction and processing," *J. Acoust. Soc. Am.*, vol. 88, no. 5, pp. 2248–2258, Nov., 1990
[9] J. V. Candy, R. W. Ziolkowski, and D. K. Lewis, "Transient wave estimation: A multichannel deconvolution application," *J. Acoust. Soc. Amer.*, vol. 88, no. 5, pp. 2235–2247, Nov., 1990
[10] R. W. Ziolkowski and D. K. Lewis, "Verification of the localized wave transmission effect," *J. Appl. Phys.*, vol. 68, no. 12, pp. 6083–6086, Dec. 15, 1990
[11] J. Durnin, "Exact solutions for nondiffracting beams—I: The scalar theory," *J. Opt. Soc.*, vol. 4, no. 4, pp. 651–654, 1987
[12] J. Durnin, J. J. Miceli, Jr., and J. H. Eberly, "Diffraction-free beams," *Phys. Rev. Lett.*, vol. 58, no. 15, pp. 1499–1501, Apr. 13, 1987
[13] F. Bloisi and L. Vicari, "Comparison of nondiffracting laser beams," *Optics Commun.*, vol. 75, nos. 5 and 6, pp. 353–357, Mar. 15, 1990.
[14] G. Indebetow, "Nondiffracting optical fields: some remarks on their analysis and synthesis," *J. Opt. Soc. Amer. A*, vol. 6, no. 1, pp. 150–152, Jan., 1989
[15] F. Gori, G. Guattari, and C. Padovani, "Model expansion for J_0-correlated Schell-model sources," *Optics Commun.*, vol. 64, no. 4, pp. 311–316, Nov. 15, 1987
[16] K. Uehara and H. Kikuchi, "Generation of near diffraction-free laser beams", *Appl. Phys. B*, vol. 48, pp. 125–129, 1989
[17] L. Vicari, "Truncation of nondiffracting beams," *Optics Commun.*, vol. 70, no. 4, pp. 263–266, Mar. 15, 1989
[18] M. Zahid and M. S. Zubairy, "Directionally of partially coherent Bessel–Gauss beams," *Optics Commun.*, vol. 70, no. 5, pp. 361–364, Apr. 1, 1989
[19] S. Y. Cai, A. Bhattacharjee, and T. C. Marshall, " 'Direction-free' optical beams in inverse free electron laser acceleration," *Nuclear Instruments and Methods in Physics Research, Section A: Accelerators, Spectrometers, Detectors, and Associated Equipment*, vol. 272, no. 1–2, pp. 481–484, Oct., 1988
[20] D. K. Hsu, F. J. Margetan, and D. O. Thompson, "Bessel beam ultrasonic transducer: fabrication method and experimental results," *Appl. Phys. Lett.*, vol. 55, no. 20, pp. 2066–2068, Nov. 13, 1989
[21] J.-Y. Lu and J. F. Greenleaf, "Ultrasonic nondiffracting transducer for medical imaging," *IEEE Trans. Ultrason., Ferroelec, Freq. Contr.*, vol. 37, pp. 438–447, Sept., 1990
[22] ——, "Pulse-echo imaging using a nondiffracting beam transducer," *US Med. Biol.*, vol. 17, no. 3, pp. 265–281, May, 1991
[23] ——, "Evaluation of a nondiffracting transducer for tissue characterization," *1990 IEEE Ultrason. Symp. Proc.*, Honolulu, HI, vol. 2, pp. 795–798, Dec. 4–7, 1990.
[24] ——, "A computational and experimental study of nondiffracting transducer for medical ultrasound," *Ultrason. Imag.*, vol. 12, no. 2, pp. 146–147, Apr. 1990 (abst)
[25] ——, "Simulation of imaging contrast of nondiffracting beam transducers," *J. Ultrasound Med.*, vol. 10, no. 3 (suppl), p. S4, Mar. 1991 (abst).
[26] J. A. Campbell and S. Soloway, "Generation of a nondiffracting beam with frequency independent beam width," *J. Acoust. Soc. Amer.*, vol. 88, no. 5, pp. 2467–2477, Nov. 1990.
[27] J.-Y. Lu, and J. F. Greenleaf, "Nondiffracting X waves—exact solutions to free-space scalar wave equation and their finite aperture realizations," *IEEE Trans. Ultrason. Ferroelec., Freq. Contr.*, vol. 39, pp. 19–31, Jan. 1992.
[28] J. W. Goodman, *Introduction to Fourier Optics.* New York: McGraw-Hill, 1968, chs. 2–4
[29] A. V. Oppenheim and R. W. Schafer, *Digital Signal Processing.* Englewood Cliffs, NJ: Prentice-Hall, 1975, ch. 5
[30] J.-Y. Lu and J. F. Greenleaf, "Theory and acoustic experiment of nondiffracting X waves," *1991 IEEE Ultrason. Symp. Proc.*, Lake Buena Vista, FL, Dec. 8–11, 1991, in press.

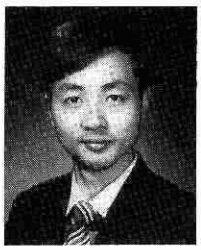

Jian-yu Lu (M'88), was born in Fuzhou, Fujian Province, People's Republic of China, on August 20, 1959. He received the B.S. degree in electrical engineering in 1982 from Fudan University, Shanghai, China, the M.S. degree in 1985 from Tongji University, Shanghai, China, and the Ph.D. degree from Southeast University, Nanjing, China.

He is currently an Associate Consultant at the Biodynamics Research Unit, Department of Physiology and Biophysics, Mayo Clinic and Foundation, Rochester, MN, and he is an Assistant Professor of Biophysics at the Mayo Medical School. Previously, he was a Research Associate at the Biodynamics Unit, and from 1988 to 1990, he was a postdoctoral Research Fellow. Prior to that, he was a Faculty Member of the Department of Biomedical Engineering, Southeast University, and worked with Prof. Yu Wei. His research interests are in acoustical imaging and tissue characterization, medical ultrasonic transducers, and nondiffracting wave transmission.

Dr. Lu is a member of the IEEE UFFC Society, the American Institute of Ultrasound in Medicine, and Sigma Xi.

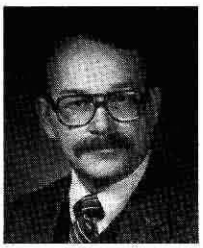

James F. Greenleaf (M'73–SM'84–F'88) was born in Salt Lake City, UT, on February 10, 1942. He received the B.S. degree in engineering science in 1968 from Purdue University, West Lafayette, IN, and the Ph.D. degree in engineering science in 1970 from the Mayo Graduate School of Medicine, Rochester, MN, and Purdue University.

He is a Professor of Biophysics and Medicine at the Mayo Medical School, and a Consultant at Biodynamics Research Unit, Department of Physiology, Biophysics, and Cardiovascular Disease and Medicine, Mayo Foundation.

Dr. Greenleaf has served on the IEEE Technical Committee of the Ultrasonics Symposium since 1985. He served on the IEEE-UFFC Subcommittee for the Ultrasonics in Medicine/IEEE Measurement Guide Editors, and on the IEEE Medical Ultrasound Committee. He is the President of the IEEE UFFC Society. He holds five patents and is the recipient of the 1986 J. Holmes Pioneer Award from the American Institute of Ultrasound in Medicine, and he is a Fellow of the IEEE and of the AUIM. He is the Distinguished Lecturer for the IEEE UFFC Society for 1990–1991. His special field of interest is in ultrasonic biomedical imaging science and has published more than 150 articles and edited four books.